

AD-A114 165

NAVAL RESEARCH LAB WASHINGTON DC
SPOT SPECTROSCOPY: LOCAL SPECTROSCOPIC MEASUREMENTS WITHIN LASE--ETC(U)
APR 82 M J HERBST, P G BURKHALTER, J GRUN
NRL-MR-4812

F/G 20/9

UNCLASSIFIED

NL

1-1
A-114

END
DATE
FILMED
5 82
DTIC

AD A114165

REPORT DOCUMENTATION PAGE		READ INSTRUCTIONS BEFORE COMPLETING FORM
1. REPORT NUMBER NRL Memorandum Report 4812	2. GOVT ACCESSION NO. DA114 165	3. RECIPIENT'S CATALOG NUMBER
4. TITLE (and Subtitle) SPOT-SPECTROSCOPY: LOCAL SPECTROSCOPIC MEASUREMENTS WITHIN LASER-PRODUCED PLASMAS		5. TYPE OF REPORT & PERIOD COVERED Interim report on a continuing NRL problem.
		6. PERFORMING ORG. REPORT NUMBER
7. AUTHOR(s) M.J. Herbst, P.G. Burkhalter, J. Grun*, R.R. Whitlock, and M. Fink**		8. CONTRACT OR GRANT NUMBER(s)
9. PERFORMING ORGANIZATION NAME AND ADDRESS Naval Research Laboratory Washington, DC 20375		10. PROGRAM ELEMENT, PROJECT, TASK AREA & WORK UNIT NUMBERS 47-0859-0-2
11. CONTROLLING OFFICE NAME AND ADDRESS U.S. Department of Energy Washington, DC 20545		12. REPORT DATE April 20, 1982
		13. NUMBER OF PAGES 17
14. MONITORING AGENCY NAME & ADDRESS (if different from Controlling Office)		15. SECURITY CLASS. (of this report) UNCLASSIFIED
		15a. DECLASSIFICATION/DOWNGRADING SCHEDULE
16. DISTRIBUTION STATEMENT (of this Report) Approved for public release; distribution unlimited.		
17. DISTRIBUTION STATEMENT (of the abstract entered in Block 20, if different from Report)		
18. SUPPLEMENTARY NOTES *Present address: Mission Research Corporation, Alexandria, VA 22312 **Present address: Sachs/Freeman Associates, Bowie, MD 20715 This work was supported by the U.S. Department of Energy and the Office of Naval Research.		
19. KEY WORDS (Continue on reverse side if necessary and identify by block number) X-ray spectroscopy Laser-plasma interactions Plasma diagnostics		
20. ABSTRACT (Continue on reverse side if necessary and identify by block number) Use of a locally embedded tracer in laser-irradiated solid targets yields a localized source of diagnostic x-ray line radiation in the blowoff plasma. This technique potentially eliminates problems of chord-integration over regions of varying density and temperature in an inhomogeneous plasma, and reduces complications due to plasma opacity effects in the interpretation of spectra. Spectra obtained in an experimental test of this new technique are of a quality superior to those obtained from standard laser-produced plasmas, and should provide the best tests to date of spectroscopic models for these plasma conditions.		

DD FORM 1 JAN 73 1473

EDITION OF 1 NOV 65 IS OBSOLETE
S/N 0102-014-6601

SECURITY CLASSIFICATION OF THIS PAGE (When Data Entered)

CONTENTS

INTRODUCTION	1
EXPERIMENTAL TECHNIQUES	2
A. Target Fabrication	2
B. The Proof-of-Principle Experiment	3
C. In-Situ Measurements of Spectrograph Magnification	5
RESULTS AND DISCUSSION	6
A. Results of Experiment and Comparison of Techniques	6
B. Caveats and Remaining Questions	10
CONCLUSIONS	12
ACKNOWLEDGMENTS	13
REFERENCES	14



Accession For	
NTIS GRA&I	<input checked="" type="checkbox"/>
DTIC TAB	<input type="checkbox"/>
Unannounced	<input type="checkbox"/>
Justification	
By _____	
Distribution/	
Availability Codes	
Dist	Avail and/or Special
A	

SPOT SPECTROSCOPY: LOCAL SPECTROSCOPIC MEASUREMENTS WITHIN LASER-PRODUCED PLASMAS

INTRODUCTION

Density and temperature profiles are directly related to energy absorption and transport processes in plasmas produced by laser irradiation of solid targets. Therefore, measurements of these plasma parameters play a central role in experiments addressing the physics relevant to laser-driven nuclear fusion.¹ At the densities and temperatures of interest, x-ray spectroscopy provides one viable method for performing these measurements.^{2,3}

There are two major drawbacks to the use of standard spectroscopic techniques in these plasmas. First, the measurements are integrated along a diagnostic line-of-sight through an inhomogeneous plasma. Second, effects of plasma opacity on the radiation exiting the plasma are non-negligible at the higher densities of interest.^{4,5} One could use straightforward inversion techniques to obtain spatially resolved emissivities from the chord-integrated data if the plasmas were optically thin and axisymmetric,³ but the additional complication of spatially varying opacity makes inversion much more difficult. More typically, one predicts the plasma profile using a hydrodynamics computer code and compares the experimentally observed spectrum with those calculated for chord-integrations across the inhomogeneous plasma.^{6,7} One is dependent in that case upon the correctness of the hydrodynamics model as well as the atomic physics model; one would obviously prefer to make direct determinations of density and temperature, independently of the hydrodynamics.

In the present work, a new spectroscopic method is described which circumvents the problem of plasma inhomogeneity and reduces the effects of plasma opacity. Spot spectroscopy, the new technique, differs from standard spectroscopic techniques in that the source of diagnostic radiation

Manuscript submitted March 5, 1982.

is locally embedded into the solid target before laser-irradiation. As recently demonstrated,⁸ the tracer material which is ablated by the laser can be confined collisionally in the hydrodynamic flow from the target; this yields a source of diagnostic lines which is localized within the blowoff plasma. In Sec. I, we explain the target fabrication procedure and describe a method for in-situ measurement of the spectrograph magnification. Data obtained with the new technique are compared with standard spectroscopic data in Sec. II, which also contains a discussion of caveats and remaining questions. Finally, we assess the new technique in Sec. III.

I. EXPERIMENTAL TECHNIQUES

A. Target Fabrication

For the proof-of-principle experiment, we choose polystyrene targets with embedded aluminum tracers. The tracer is so chosen because collisional radiative equilibrium (CRE) computer models suggest the utility of aluminum lines for measurement of temperatures and densities of interest.⁹ The polystyrene is chosen because it is a common and easily fabricated target material. Also, its lower atomic number Z increases the ratio of the aluminum tracer emission to the surrounding plasma emission and reduces the opacity of the surrounding plasma to the tracer emission.

A two-step process is used to fabricate these targets. The first step is the evaporation of the tracer material onto a soaped-glass substrate using the standard technique of vacuum evaporation from a hot filament source. The thin film of TEEPOL 610 detergent¹⁰ on the glass prevents the aluminum from adhering better to the glass than it will to the polystyrene. To achieve local deposition of the aluminum, bi-metal masks into which the desired patterns have been chemically etched are magnetically clamped in

intimate contact with the glass substrate; for the present experiment, these patterns are circular spots of various diameters. In the second step of the process, polystyrene dissolved in butyl acetate is cast over the aluminum-coated glass substrate. When dry, the composite is lifted and the aluminum is embedded in the polystyrene; the surface of the tracer is flush with that of the plastic.

B. The Proof-of-Principle Experiment

Except for the presence of the tracer in the target, the experimental arrangement for the new technique is much the same as for standard x-ray spectroscopy. As shown in Fig. 1, the targets are irradiated with 50-250J of Nd laser radiation (1.054 μm wavelength) in a 4-5 nsec pulse. We choose to operate at two focal conditions for this experiment. First, at the best focus of our f/6 input lens, we use focal diameters (90% laser energy content) near 100 μm , and spatially averaged irradiances up to $5 \times 10^{14} \text{ W/cm}^2$. Because larger focal diameters are required to minimize edge effects in planar experiments, targets are also placed in the quasi-near field of the focusing lens; intensities between 10^{12} and 10^{13} W/cm^2 are obtained with focal diameters of 800-1000 μm .

The aluminum line radiation in the 5-8 \AA spectral region is detected using an x-ray crystal spectrograph with a viewing axis parallel to the target surface. Spectral dispersion is achieved through use of a PET crystal, and spatial resolution in the direction on the film which is orthogonal to the spectral dispersion is accomplished with an entrance slit. As shown in Fig. 1, the slit is oriented to yield spatial resolution in the direction along the laser axis; resolution in the other two spatial dimensions results from the knowledge of the position of the localized

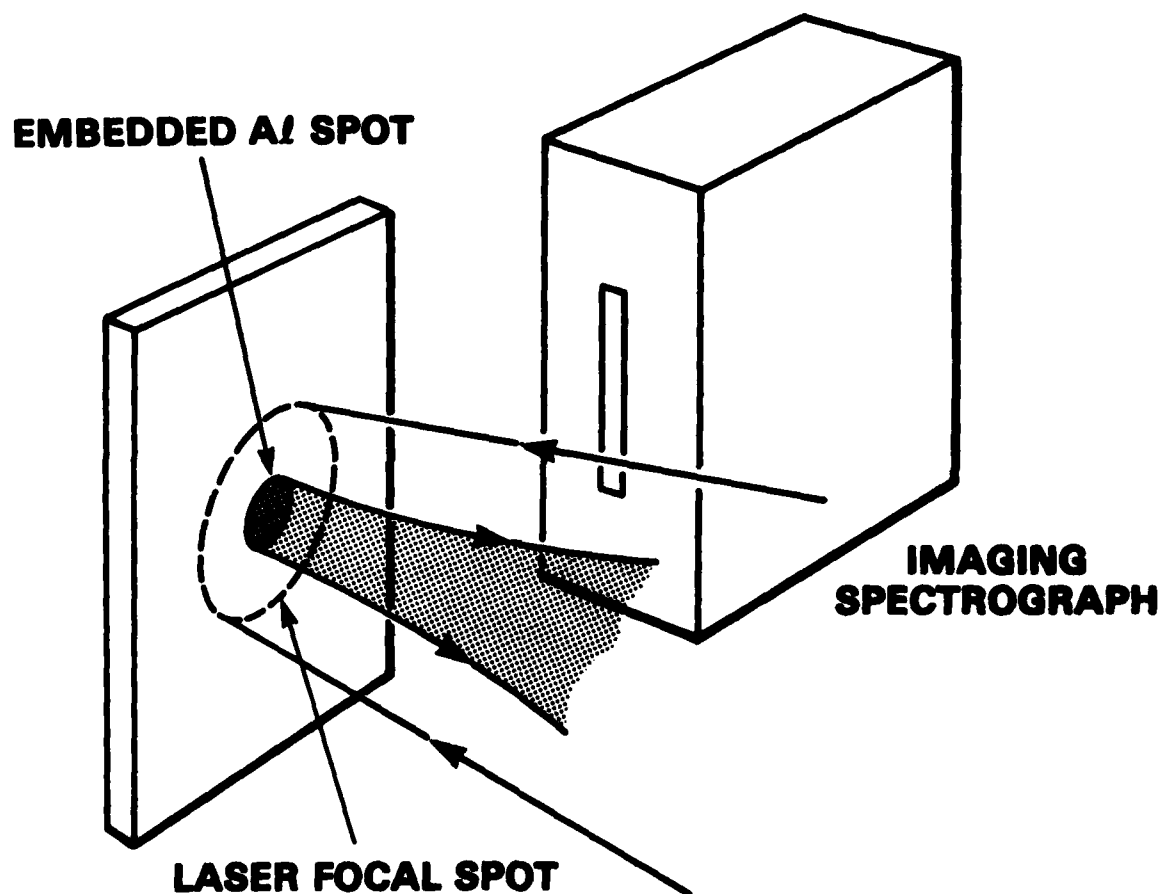


Fig. 1 — Experimental configuration for spot spectroscopy

tracer within the focal spot. The slit is located 4-5mm from the target, which represents a tradeoff between light collection efficiency and slit survivability; even at this distance, the 25 μm thick nickel slit substrate is occasionally destroyed by target debris during a laser shot. Another compromise must often be made between spatial resolution and detectability of relevant spectral lines. To improve spatial resolution along the laser axis, one must reduce the slit width, sacrificing spectral intensity; to recover the spectral intensity, one may choose to increase the implanted spot diameter, reducing spatial resolution in the other two dimensions. For the purposes of this study, slit widths between 4 and 30 μm and tracer spot diameters between 40 and 250 μm are used. The spectra are recorded on Kodak No-Screen film, for which a film model¹¹ based upon an absolute calibration¹² is available. A beryllium filter of nominally 15 μm thickness protects the film from visible exposure.

C. In-Situ Measurements of Spectrograph Magnification

In principle, one may use the measured slit-to-film and slit-to-source distances to calculate the magnification of the spectrograph. However, given the uncertainties with which the exact paths of diffracted rays of various wavelengths can be measured, we prefer a direct in-situ measurement of the spectrograph magnification.

To measure the magnification in situ, we devised a special double target. An aluminum foil is placed in the usual target position, mounted to a glass substrate to prevent target bowing. A few hundred microns in front of the Al foil, toward the laser, a foil of copper backed by glass is mounted. The foils are aligned so that part of the incident laser beam strikes the edge of the Cu foil, producing Cu line emission, while the rest misses the Cu and propagates the additional distance to the Al surface.

The spectrograph image then contains Cu and Al lines, but the Al lines extend beyond the end of the Cu lines by a distance $L' = ML$ corresponding to the distance L between the two target foils multiplied by the spectrograph magnification M . As L may be accurately measured under a microscope, M is experimentally determined by the measurement of L' .

One potential complication with this procedure arises unless the spectrograph axis is closely aligned with the target surface; if it is not, the observed separation between the Cu and Al may be lessened due to geometrical foreshortening. To assure that this is not a problem, we add a flag to the target, a 2mm wide and 125 μ m thick glass strip on the side between the irradiated target and the spectrograph slit. This flag is offset toward the laser from the Cu surface and is mounted with its broad face parallel to the Cu and Al target surfaces. Given its location, it casts a shadow on the spectrograph; this shadow is observed on the spectrum as a gap in the Al and Cu spectral lines. By comparing the dimension of this gap with the thickness of the flag, the angle at which the flag and, therefore, the targets are viewed can be determined; any angular misalignment causes an increase in the shadow dimension which depends on the known flag width.

II. RESULTS AND DISCUSSION

A. Results of Experiment and Comparison of Techniques

To allow a comparison to be made between spot spectroscopy and standard spectroscopic techniques, we use both simple Al foil targets and CH targets with embedded Al spots. A pinhole camera filtered to detect photons with energy $h\nu \geq 1$ keV looks at the blowoff plasma along the same axis but from a position diametrically opposite the spectrograph.

Typical images of an aluminum foil plasma, obtained with a pentagonal array of pinholes with diameters between 5 and 55 μm , are shown in Fig. 2A. An x-ray spectrum obtained with an aluminum foil target can be seen in Fig. 2B, although for somewhat different conditions than apply for Fig. 2A. The horizontal edge at the bottom of the spectrum is the target surface, from which regions of strong line emission extend over distances of several hundred microns.

The x-ray pinhole images and spectrum for a CH target with embedded Al can be seen in Figs. 2C and 2D, respectively; this data is analogous to that shown in Figs. 2A and 2B for an aluminum foil target. Note that Figs. 2C and 2D are obtained on the same data shot, but that the conditions of this shot do not exactly correspond with those of either Fig. 2A or 2B. The comparison between the techniques, therefore, is qualitative rather than quantitative.

Inspection of the pinhole camera images reveals that, indeed, the source volume for the Al x-ray emission can be significantly reduced through the use of a CH target with an embedded Al spot. As expected on the basis of Ref. 8, a collisionally confined channel of aluminum flow from the embedded tracer can be identified as the track of stronger x-ray emissivity in the images of Fig. 2C. This is a much smaller source volume than the aluminum foil plasma in Fig. 2A (the 20% difference in laser focal spot diameter between Figs. 2A and 2C is not a major factor in this reduction). Even larger reductions in source size are observed when smaller embedded spots are used. To date, we have embedded spots as small as 25 μm in diameter,⁸ a limit imposed by the availability of masks for tracer evaporation. In principle, the ultimate limit is set by the ability of the plasma to collisionally confine the tracer; as ion-ion mean-free-paths are

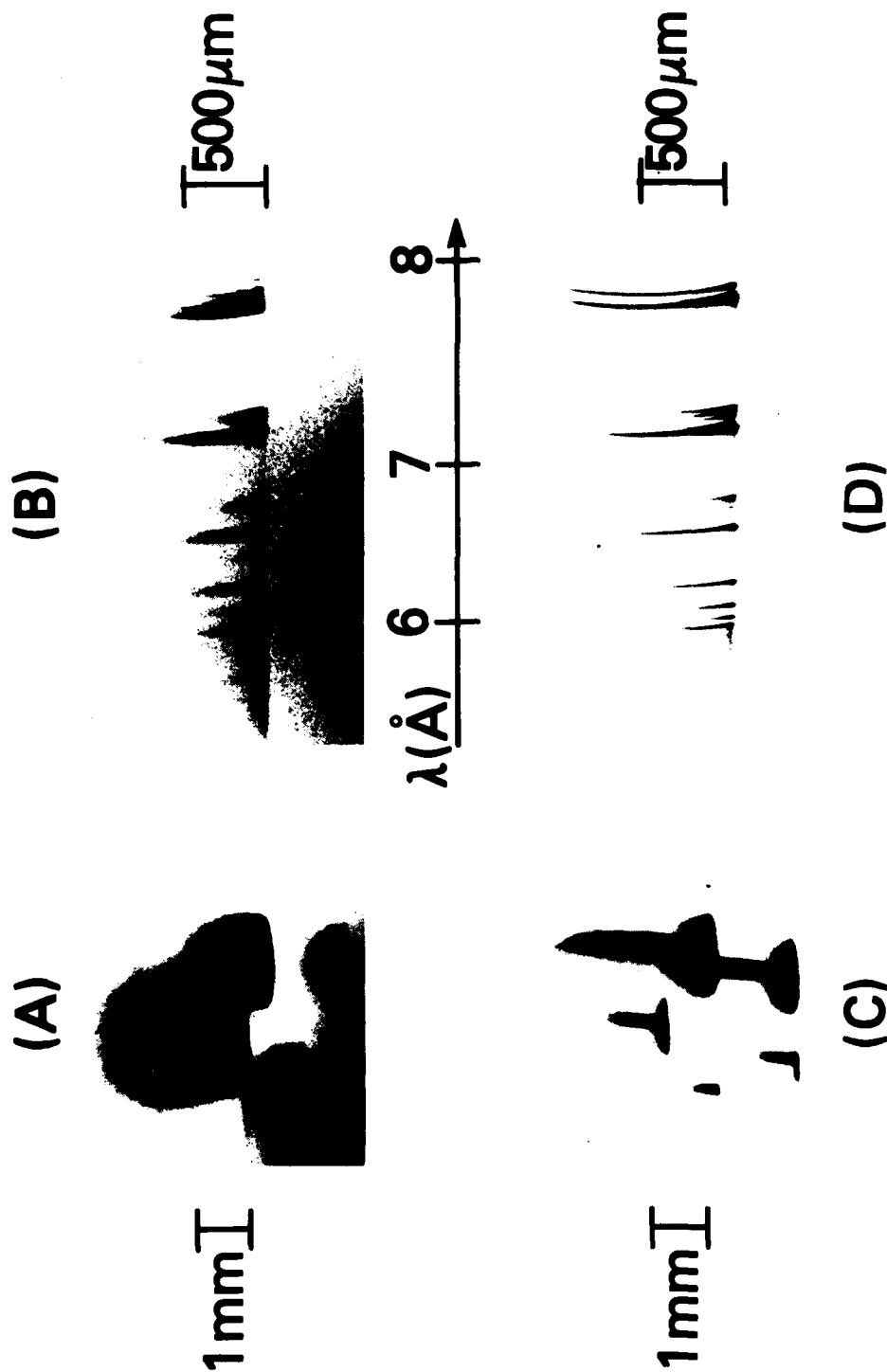


Fig. 2 — Qualitative comparison between data obtained with Al foil target and data acquired using CH plastic target locally embedded with Al. The vertical axis for (A) through (D) corresponds to the laser axis, with the laser incident from above and the target surface at bottom. (A) is obtained with Kodak 3490 film, and (B) through (D) are on Kodak No-Screen Film. A) X-ray pinhole camera images, obtained with an array of pinholes (5-55 μm diameter), for an Al foil target. Laser intensity $I_0 \approx 3 \times 10^{12} \text{ W/cm}^2$, due to 100J focused to 1100 μm diameter spot (90% energy content). (B) Spectrum obtained for Al foil target at $I_0 \approx 8 \times 10^{12} \text{ W/cm}^2$, with 110J focused to 600 μm diameter spot. (C) Pinhole images as in (A), but for CH target embedded with 180 μm diameter Al spot. 225J of laser energy focused to 900 μm diameter spot yields $I_0 \approx 8 \times 10^{12} \text{ W/cm}^2$. (D) Spectrum from same shot as (C).

estimated to be less than 1 μm even at electron densities down to 10% of critical density for the incident laser, there is considerable room for further source reduction.

A dramatic improvement in spectral resolution results from the reduction in source volume. With an Al foil target, as in Fig. 2B, the spectral widths of the lines near the target surface are quite broad; the widths exceed those expected for other broadening mechanisms, and reflect source broadening due to the large Al plasma extent transverse to the laser axis. In contrast, line widths near the target surface are much narrower, as in Fig. 2D, when a CH target with embedded Al is used. Several sets of lines which appear to the naked eye to be totally unresolved in Fig. 2B are clearly isolated in Fig. 2D. These data are obtained with the larger focal spot; a similar effect is observed at the smaller focal spot.

Two other important results of the reduced source volume are that the effects of plasma inhomogeneity can be virtually eliminated and that the effect of plasma opacity can be greatly reduced. Without embedded tracers, one might try to minimize inhomogeneity and opacity effects by reducing the size of the plasma to be studied. For laser-produced plasmas, this would be accomplished by minimizing the laser focal diameter. One could not expect, however, to approach the small plasma sizes which seem possible with embedded tracers. Even if one could localize the laser energy to micron scales, lateral transport of energy by plasma processes would tend to broaden the spectroscopic source, increasing the effect of plasma opacity. Additionally, this source would still have problems due to its inhomogeneity; one would still be sampling regions of widely different density and/or temperature. With the plasma resulting from an embedded tracer, one can hope to obtain not only very small source-plasma

diameter, minimizing opacity effects, but also a nearly homogeneous source, since the embedded spot diameter can be made much smaller than the irradiated focal diameter. The reduction in opacity, of course, is realized only if the tracer is embedded in a target material with lower opacity than the tracer at the wavelengths of interest.

Given that the source volume for emission is much smaller with the embedded Al tracer than for an Al foil, one might have anticipated greater problems with detectability of the spectrum than were actually encountered. In Fig. 2D, the spectral lines are detectable several hundred microns from the target surface, just as far as they are in the spectrum shown for the pure Al target (though under somewhat different conditions) in Fig. 2B. In fact, even continuum emission is detectable near the target surface in Fig. 2D; this continuum is not observable when plastic targets without the embedded spots are irradiated, indicating that the source of the continuum is the Al tracer material. For the stronger lines in the spectrum, such as the helium-like and hydrogen-like resonance lines ($1s^2\ ^1S_0 - 1s2p\ ^1P_1$ and $1s - 2p$, respectively) and the helium-like inter-combination line ($1s^2\ ^1S_0 - 1s2p\ ^3P_1$), exposures near the target surface tend to saturate the film except on shots where smaller embedded spots (40 μm diameter) and narrower slits (4 μm wide) are used. Weaker spectral lines such as the higher Rydberg members are lost in this limit. Spot spectroscopy does appear to be practicable, then, at least with laser energies comparable to ours.

B. Caveats and Remaining Questions

Spot spectroscopy has advantages over standard spectroscopic techniques in laser produced plasmas; however, there are a few caveats to be mentioned.

First, source localization requires a collisional plasma. This restriction may prevent use of the technique at much higher laser intensities or at much longer laser wavelengths, where higher plasma temperatures and the generation of suprathermal ions produce longer ion-ion mean-free-paths, destroying the confinement of the embedded tracer. Of course, spot spectroscopy is not limited to laser-produced plasmas; any method such as ion-beam irradiation or electrical discharge which creates collisional plasma from an initially solid target may be used to generate the spectroscopic source.

A second caveat concerns the ability of the technique to serve as a plasma diagnostic. If we are to regard the plasma flowing from the embedded tracer as a local spectroscopic probe for density and temperature measurements, then we want to be certain that conditions in the tracer plasma correspond to those in the surrounding plasma. Certainly, the visualizations of the hydrodynamic flow pattern, as shown in Ref. 8, strongly suggest that there is pressure equilibrium between Al tracers and CH plasmas. In the future we will determine by comparison with other diagnostics when there is also density and temperature equilibration.

Even if equilibration is shown for the present data, spectroscopic models show that each tracer element may be used only within limited ranges of density and temperature;⁹ to diagnose a wide range of parameters, one must use a variety of tracer materials.¹³ The required equilibration must be demonstrated for each of these diagnostic elements.

Another issue is the effect of time-integration upon the data. Much as with chord-integration, time-integration can complicate interpretation of the spectra if plasma parameters are varying during the x-ray emission. In the present experiments, we believe that the laser pulse is varying

sufficiently slowly so that the plasma profiles are nearly in a steady state during the x-ray emission. Experimental evidence¹⁴ for this is provided by streak photography of imaged $3/2 \omega_0$ emission (where ω_0 is the incident laser frequency), which indicates that the location of the $n_c/4$ surface, and therefore all higher density surfaces, is nearly steady for a few nanoseconds around the peak of the laser pulse (when the x-ray emission is observed to occur¹⁵). Even though we believe time-integration effects to be minimal for our case, one can hope to obtain time resolution with spot spectroscopy in one of two ways. First, one may replace the film with an x-ray streak camera to obtain a time-history on a single shot, though one cannot simultaneously obtain the complete spectrum of wavelengths λ for all positions z relative to the target surface. An alternative method is to deposit a tracer of lesser thickness at a prescribed depth beneath the surface of the target (this involves a more difficult, though realizable, target fabrication procedure). By varying the depth d and thickness t of the tracer, one controls the time interval during which tracer emission occurs. On a single shot, then, one obtains information for all λ and z , but at only a single time; t and d are varied on a shot-to-shot basis to generate a time history.

III. CONCLUSIONS

The advantages of the new technique are clear for measurements of density and temperature profiles in plasmas created by Nd-laser interaction with solid targets. Localization of the source of line radiation allows spectroscopic measurements to be made with three dimensions of spatial resolution. Since this alleviates the problem of chord-integration over regions of widely varying density and temperature, one generally will not need to account for the

profile along which one is integrating in order to obtain agreement with spectroscopic models.⁵ Therefore, the new technique also provides improved checks of spectroscopic models. As added bonuses: 1) the reduced source broadening improves spectral resolution in the data obtained, and 2) the interpretational problems raised by opacity effects in the plasma are much reduced, especially if the surrounding target material has much lower Z than the tracer.

The present work represents a significant step toward obtaining improved measurements of density and temperature in laser-produced plasmas. Detailed analysis of the present data, including extensive comparisons with spectroscopic models, is the subject of a future work. Further experiments are also required to fully answer all of the questions raised in Sec. IIB.

IV. ACKNOWLEDGMENTS

Valuable discussions are acknowledged with Drs. D. Duston, D. Matthews, B.H. Ripin and H. Griem. The expert technical assistance of N. Nocerino, L. Seymour, and E. Turbyfill is also greatly appreciated. This work was supported by the U.S. Department of Energy and the Office of Naval Research.

REFERENCES

1. J. Nuckolls, L. Wood, A. Thiessen, and G. Zimmerman, *Nature* 239, 139 (1972).
2. W. Lochte-Holtgreven, in Plasma Diagnostics, ed. by W. Lochte-Holtgreven (Wiley Interscience, New York, 1968), pp. 190 ff.
3. H.R. Griem, Plasma Spectroscopy (McGraw-Hill, New York, 1964).
4. D. Duston and J. Davis, *Phys. Rev.* 21A, 932 (1980).
5. J.P. Apruzese, P.C. Kepple, K.G. Whitney, J. Davis, and D. Duston, *Phys. Rev.* 24A, 1001 (1981).
6. D. Duston, J. Davis, and P.C. Kepple, *Phys. Rev.* 24A, 1505 (1981).
7. K.G. Whitney and P.C. Kepple, *J. Quant. Spectrosc. Radiat. Transfer* (accepted for publication).
8. M.J. Herbst and J. Grun, *Phys. Fluids* 24, 1917 (1981).
9. D. Duston and J. Davis, *Phys. Rev.* 21A, 1664 (1980).
10. Manufactured by Shell Oil Co. Reference to a company or product name does not imply approval or recommendation of the product by the U.S. Naval Research Laboratory or its contractors to the exclusion of others that may be suitable.
11. D.B. Brown, J.W. Criss, and L.S. Birks, *J. Appl. Phys.* 47, 3722 (1976).
12. C.M. Dozier, D.B. Brown, L.S. Birks, P.B. Lyons, and R.F. Benjamin, *J. Appl. Phys.* 47, 3732 (1976).
13. V.A. Boiko, S.A. Pikuz, and A. Ya Faenov, *J. Phys. B.* 12, 1889 (1979).
14. M.J. Herbst, J.A. Stamper, R.H. Lehmberg, R.R. Whitlock, F.C. Young, J. Grun, and B.H. Ripin, to appear in *Proceedings of the 1981 Topical Conference on Symmetry Aspects of Inertial Fusion Implosions*, ed. by S. Bodner, NRL.

15. B.H. Ripin, R. Decoste, S.P. Obenschain, S.E. Bodner, E.A. McLean,
F.C. Young, R.R. Whitlock, C.M. Armstrong, J. Grun, J.A. Stamper,
S.H. Gold, D.J. Nagel, R.H. Lehmberg, and J.M. McMahon, Phys. Fluids
23, 1012 (1980), and 24, 990 (1981).

**DAI
FILM**